FISEVIER

Contents lists available at ScienceDirect

Bioresource Technology

journal homepage: www.elsevier.com/locate/biortech



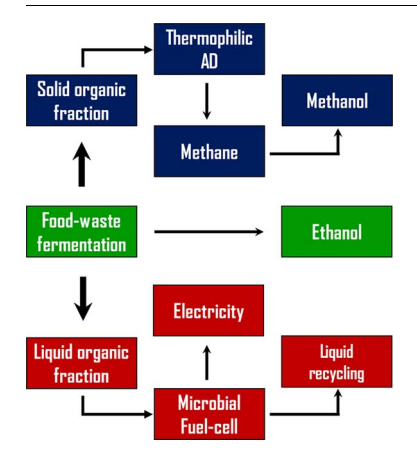
Producing methane, methanol and electricity from organic waste of fermentation reaction using novel microbes



Saurabh Sudha Dhiman^{a,b,c}, Namita Shrestha^d, Aditi David^a, Neha Basotra^{a,e}, Glenn R. Johnson^f, Bhupinder S. Chadha^e, Venkataramana Gadhamshetty^{b,d,g}, Rajesh K. Sani^{a,b,c,*}

- a Department of Chemical and Biological Engineering, South Dakota School of Mines and Technology, Rapid City, SD 57701, USA
- ^b BuG ReMeDEE Consortium, South Dakota School of Mines and Technology, Rapid City, SD 57701, USA
- ^c Composite and Nanocomposite Advanced Manufacturing Centre Biomaterials (CNAM/Bio), Rapid City, SD 57701, USA
- d Department of Civil and Environmental Engineering, South Dakota School of Mines and Technology, Rapid City, SD 57701, USA
- ^e Department of Microbiology, Guru Nanak Dev University, Amritsar, Punjab 143005, India
- f Hexpoint Technologies Inc. PO Box 1159, Panama City, FL 32402, USA
- ⁸ Surface Engineering Research Centre, South Dakota School of Mines and Technology, Rapid City, SD 57701, USA

GRAPHICAL ABSTRACT



ARTICLE INFO

Keywords:
Food waste
Methane oxidation
Methyloferula stellata
Microbial fuel cell
Thermophilic anaerobic digestion

ABSTRACT

Residual solid and liquid streams from the one-pot CRUDE (Conversion of Raw and Untreated Disposal into Ethanol) process were treated with two separate biochemical routes for renewable energy transformation. The solid residual stream was subjected to thermophilic anaerobic digestion (TAD), which produced 95 ± 7 L methane kg $^{-1}$ volatile solid with an overall energy efficiency of $12.9 \pm 1.7\%$. A methanotroph, *Methyloferula* sp., was deployed for oxidation of mixed TAD biogas into methanol. The residual liquid stream from CRUDE process was used in a Microbial Fuel Cell (MFC) to produce electricity. Material balance calculations confirmed the integration of biochemical routes (i.e. CRUDE, TAD, and MFC) for developing a sustainable approach of energy regeneration. The current work demonstrates the utilization of different residual streams originated after food waste processing to release minimal organic load to the environment.

^{*} Corresponding author at: Department of Chemical and Biological Engineering, South Dakota School of Mines and Technology, Rapid City, SD 57701, USA. E-mail address: Rajesh.sani@sdsmt.edu (R.K. Sani).

1. Introduction

The US Energy Security and Independence Act of 2007 (Department of Energy and Department of Agriculture) mandates the use of biomass to supply 5% of heat and electricity sources, 20% of transportation fuel, and 25% of value-added products by 2022 (Perlack et al., 2015). Currently, 13% of the renewable energy portfolio in the US is covered by liquid biofuels including ethanol and diesel. Results from a series of recent studies support the use of biorefinery concepts to convert renewable feedstocks into liquid transportation fuels (Dhiman et al., 2016). Transformative biorefinery technologies can yield innovative solutions for challenges related to energy security, the environment, and rural development (Dhiman et al., 2015).

A criticism of crop-based biofuel production is that it requires land and water that could otherwise be used for production of typical agricultural food products, special commodities, and fiber (Michel, 2012). Another negative aspect of energy-crop based biorefinery is the lower values for photosynthetic efficiency and their carbon-neutral capacity compared to food-crops (Lin et al., 2013). Food waste (FW), a nutrient rich and abundant feedstock (up to 43.6 million tons per year in US), is an alternative to agricultural commodities as feedstocks for renewable energy production (Gustavsson et al., 2011). The FW contains soluble sugars and polymers (FAO, 2015), which can act as precursors for high-value commercial compounds as well as energy source, thus making FW as valuable feedstock in the biorefinery (Rosentrater, 2006).

The goal of a biorefinery is to produce renewable energy and valueadded products from a given feedstock in a timely and energy-efficient manner (Dhiman et al., 2017a). In order to be cost-effective, commercial biofuel production must overcome several economic and technical challenges. The majority energy requirements for an integrated biorefinery process emerge from the five core steps: feedstock collection, pretreatment of the feedstock, hydrolysis of the bulk feedstock, fermentation, and product separation (Koutinas et al., 2014). Some of the limitations in the biorefinery approach can be resolved by using the extremophilic microorganisms that thrive in high temperatures and other challenging operational conditions (Rahayu et al., 2017). In our previous exploration of microbes from the deep-biosphere of Sanford Underground Research Facility (SURF) (Lead, SD), several unique microbes including thermophiles have been isolated and characterized. We extended those discoveries and applied them to the development a novel biorefinery approach (CRUDE process) that uses thermophilic microbes to consolidate the core steps of waste treatment and biofuel production into a single bioprocess (Dhiman et al., 2017b).

To improve the energy efficiency and broaden the product portfolio of the CRUDE or other similar bioprocesses, the current study investigates feasibility of generating additional forms of renewable fuels (methane and methanol) and electricity from the CRUDE process effluent. The study includes energy and mass balance calculations to evaluate the feasibility of the combined biorefinery framework for treating FW and its conversion to useable bioenergy. The additional

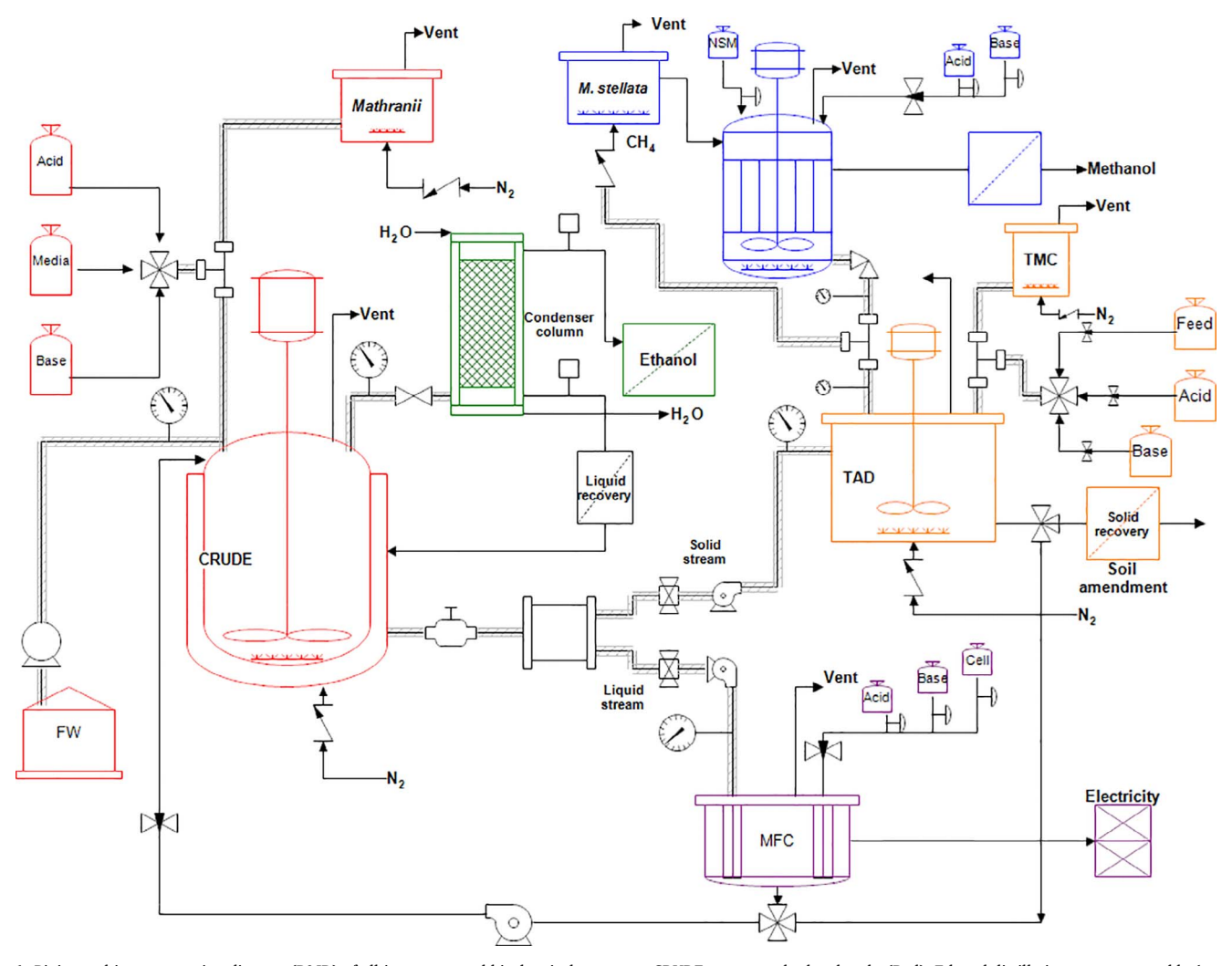


Fig. 1. Piping and instrumentation diagram (P&ID) of all interconnected biochemical processes. CRUDE reactor and related tanks (Red); Ethanol distillation process assembly (green); TAD (orange); MFC reactor (purple); and methane oxidation reactor (MOR) (blue). (For interpretation of the references to colour in this figure legend, the reader is referred to the web version of this article.)

process increases energy conversion from the secondary biological waste and reduces residual waste.

2 Materials and methods

2.1. Isolation and enrichment of thermophiles

The thermophilic methanogenic consortium (TMC) was developed at 60 °C and pH 7.0 using sludge samples collected from an anaerobic digester at the Rapid City (SD) Wastewater Reclamation Plant. The enrichment was done with mixture of food (1% w/v) and paper (0.5% w/v) waste mixed into a defined anaerobic medium. The medium contained (g L $^{-1}$): K₂HPO₄, 0.3; KH₂PO₄, 0.3; NaCl, 0.1; CaCl₂, 0.05; NH₄Cl, 1.0; MgCl₂·6H₂O 0.5; KCl, 0.3; cysteine.HCl, 0.5; yeast extract, 0.05 and Na₂S·9H₂O, 0.003. NaHCO₃ and trace element solutions (ATCC # 283) were also added to the medium to make a final concentration of 20 mM and 2.5 mL L $^{-1}$, respectively. The pH of the medium was adjusted to 7.0 using 10 M NaOH.

The microbial consortium used in microbial fuel cell (MFC) reactor was isolated and enriched as described previously (Shrestha et al., 2016). Novel deep-biosphere methanotrophs were isolated from the deep biosphere of the SURF (4850 ft. deep level). Molecular identification of isolates purified from different enrichment cultures was performed by amplifying 16S rRNA genes using bacteria specific primers 8f/1492r as described earlier (Dhiman et al., 2012, 2013). The isolate that exhibited the highest methane oxidation potential was cultured in nitrate mineral salt medium (NMS, pH 7.0) using methane gas as a sole source of carbon at 30 °C under shaking conditions (150 rpm).

2.2. Thermophilic anaerobic digestion (TAD) of solid residue

Overview of all interconnected biochemical processes viz. CRUDE reactor (red), TAD (orange), MFC (purple), methane oxidation (blue), and ethanol distillation (green) are shown in Fig. 1. After the completion of the CRUDE process, the ethanol was recovered, and different waste streams (e.g., solid and liquid wastes) were separated using centrifugation as described previously (Dhiman et al., 2017b). The CRUDE solid residual stream (CSRM) was directed towards TAD reactor containing defined growth medium (devoid of any additional carbon source) and inoculated with $2.2\,\mathrm{g\,L}^{-1}$ (dry cell weight) of TMC. Samples from head space and liquid medium were collected after every 12h for analysis of the gas composition and components left in solid residual stream.

2.3. Usage of liquid residual in microbial fuel cell (MFC)

The MFC in this study is based on the two-compartment design described in our earlier report (Shrestha et al., 2017). The operational external resistance in the MFC tests was 1000Ω throughout study. Sodium 2-bromoethanesulfonate (0.4 g L $^{-1}$, final concentration) was added to the anolyte to inhibit methanogenesis in all the MFC tests. The catholyte was phosphate buffer (50 mM, pH 7.0) and ferricyanide (50 mM) as the terminal electron acceptor. The test MFCs were evaluated under a fed-batch mode using typical monitoring, test methods, and electrochemical impedance spectroscopy procedures as described previously (Shrestha et al., 2016).

The unprocessed CRUDE effluent (UCE, liquid residual) was transferred to a mature test MFC which had been operated for 2 years. The spent anolyte from the mature test MFC was replaced with the liquid waste stream using the following steps: drain the spent anolyte from the anode, gently rinse the anode with sterile phosphate buffer, and refill the anode with an equivalent volume (180 mL) of the unprocessed crude effluent. The UCE waste stream was supplemented with minimal salts (g $\rm L^{-1}$) (NH₄Cl, 1.24; KCl, 0.52; NaH₂PO₄·H₂O, 2.45; and Na₂HPO₄·7H₂O, 4.576). The organic fraction of the UCE (i.e., devoid of any external supplements) served as the sole source of electron donor in the MFC.

2.4. Biochemical oxidation of methane to methanol

The methane oxidation experiments were conducted in batch mode with an isolated Methyloferula stellata and by using Methylosinus trichosporium OB3b as a control strain. Previously described nitrate mineral salt (NMS) medium was used for cultivating and maintaining the methanotrophs (Bowman and Sayler, 1994). Batch mode of methane oxidation was carried out using 500 mL serum bottles filled with 200 mL of NMS medium, supplemented with 30 mL of phosphate buffer (100 mM) with 10 µM of Fe(II). Under unoptimized conditions inoculum cell mass was maintained at 1.5 mg mL⁻¹. Methane gas was used as sole carbon source (mixed with air 1:1 v/v, 10 mL min⁻¹ flow rate) and cultures were incubated at 30 °C, 200 rpm for 48 h. After optimizing the operational parameters, reaction conditions were maintained at 30 °C, pH 7.0, 150 RPM for up to 24 h incubation using 1.8 g DW L⁻¹ inoculum cell mass. Liquid samples were collected periodically to measure the concentrations of methanol as described previously.

2.5. Energy calculations

The total energy recovered from the two waste streams (i.e. solid and liquid) from the CRUDE reactor was calculated separately. The energy efficiency (EE) of the TAD process was calculated using the following equation (Inglesby and Fisher, 2012).

$$EE_{TAD} = P_{methane} \cdot E_{methane} / \Delta H_{FW} \cdot m_{added}$$

Where $P_{methane}$ – volume of methane produced per day; $E_{methane}$ – energy density 35.8 kJ L $^{-1}$ CH $_4$; ΔH_{FW} – heat of combustion of solid residual; and m_{added} – volatile solids in solid residual added initially to TAD reactor.

The energy values obtained from CRUDE and TAD reactions were added to energy values of the MFC process and normalized to the energy stored within the FW derived after different processes as:

$$EE_{FW} = P_{Ethanol} \cdot SE_{Ethanol} + P_{methane} \cdot E_{methane} + E_{MFC} \cdot I_{SS} / \Delta H_{FW} \cdot m_{added}$$

Where P_{Ethanol} – concentration of ethanol; SE_{Ethanol} – specific energy of ethanol (MJ kg⁻¹); P_{methane} – produced methane (L CH₄ L⁻¹ d⁻¹); E_{methane} – energy density (35.8 kJ L⁻¹ CH₄); E_{MFC} – steady state cell voltage (V); I_{ss} – steady state current (A L⁻¹ d⁻¹); ΔH_{FW} – heat of combustion of secondary waste; and m_{added} – volatile solids in FW added to system.

2.6. Material balance of the overall process

Material balance was performed for both total mass of the developed process and for the carbon. Along with solid and liquid phases, added feed and inoculum were also included while measuring the carbon balance. Based on that, the hydrolyzed substrate fraction was calculated using equation (Hatiz et al., 1996):

$$(1-m_{\rm S/C}/m_{\rm S,0}) \times 100$$

Where $m_{s/C}$ and $m_{s,0}$ are solid contents after and before the overall biochemical process.

Solid composition was represented on a dry weight basis, while sugar concentrations are reported as monomeric equivalents. The total soluble sugar concentrations, including both monomeric and oligomeric forms, are measured in the liquid phase in gram per litre. For mass balance calculations, the compositions of solid and liquid phases were converted to carbon moles (C-mol) using information from the total mass balance and the C-mol weights of the components where C-mol is the amount of a substance containing 1 mol of elemental carbon (Roels, 1983). The cell mass was quantified in terms of dry cell mass and then converted to the appropriate concentration units (Combs and Hatzis, 1996).

2.7. Analytical studies

The concentrations of the CH₄, H₂ and CO₂ in the headspace of a TAD reactor were determined using a gas chromatography fitted with thermal conductivity detector (GC-TCD) and a Porapak-Q column (Agilent Technologies, Santa Clara, CA, USA) (Gancedo and Serrano, 1989). Ammonium ion (NH₄⁺) concentrations were measured using spectrophotometric techniques (HACH, USA) (Inglesby and Fisher, 2012). The MFC experiments, anolyte samples were collected on a daily basis using an air-tight syringe to measure pH and soluble chemical oxygen demand (sCOD) using APHA standard methods (APHA, 1999). The concentrations of fermentation metabolites (e.g., lactate, acetate, and butvrate) were determined by using HPLC (Shimadzu LC20: Columbia, MD, USA) equipped with a 300 × 7.8 mm Aminex HPX-87H column (BioRad, Hercules, CA, USA) and a refractive index detector (RID) (Vohra et al., 2015). The coulombic efficiency was calculated based on the initial and final COD concentrations during each cycle of the fed-batch operation (Logan et al., 2006). For analysis of methane oxidation products, the reaction mixture was clarified by centrifugation (8000g for 10 mins at 4°C) and then the supernatant was filtered (0.45 µm filter unit (MILLEX®-HV)) assembled in Gas chromatography (GC) (Agilent 7890A) equipped with a Flame Ionization Detector (FID) was used to confirm and then used to quantify the production of methanol. A HP-5 polyethylene glycol column (Agilent 19091J-413) was used to separate the reaction products with a mixture of helium and hydrogen as carrier gas mixture (25 mL min⁻¹).

3. Results and discussion

3.1. Characterization of microbes

Ten milliliters of effluent sample collected from anaerobic digester at Waste Water Reclamation Plant, Rapid City, SD was inoculated in 500 mL serum bottles containing 100 mL of sterilized growth medium supplemented with mixture of food waste (1%; w/v; undefined, locally collected, grinded paste) and paper waste (0.5%; w/v; unbleached, shredded paper towel). The bottles were sealed with butyl rubber stoppers and crimped with aluminum seals. The enrichments were performed by incubating the serum bottles at 60 °C in an incubator shaker (50 rpm). Triplicate serum bottles were used for each enrichment experiment and controls included were: (i) food waste samples autoclaved at 121 °C, (ii) effluent sample-free controls, and (iii) food waste source-free controls. Periodically, headspace samples were aseptically removed by syringe and needle, and analyzed for methane to measure the microorganisms' growth. Cultures showing growth (presence of methane) were subcultured more than five times into fresh medium prior to initiating the TAD experiments. Further to enrich the methanogenesis capabilities, 5% (v/v) inoculum was used from the first batch to start the TAD process in the second batch experiment. Subsequent batches were inoculated in similar manner using the inoculum from previous cycle. The mixture of food and paper waste was corresponding to 1.2-1.5~g VS/Kg-waste (dry weight). Values of organic content varies significantly according to source of waste collection. Values of organic content varies significantly according to source of waste collection. Detailed molecular characterization of the TMC is underway (manuscript in preparation).

For MFC set-up, microbial population was originally collected from primary clarifier overflow line of the Rapid City, SD wastewater reclamation facility. Enrichment step was carried out using a chemically defined minimal media that was supplemented with acetate and included 35 repeatable cycles (~over 500 days) of fed-batch mode. Ambient temperature (25 °C) and neutral pH range was maintained to run the MFC with enrich microbial population. These optimized parameters were similar to other published reports (Wu et al., 2018). Further, Illumina sequencing analysis indicated that the enriched community was based on Corynebacterium (34.43%), Bacteroides (16.67%), Shewanella (11.38%), Ruminobacillus (8.31%), Enterobacter (1.05%) and other species (28.16%). The two-year MFC operational duration provided a robust microbial consortium for waste treatment.

Phylogenetic analysis of newly isolated methanotroph confirmed more than 99% of its identity with *M. stellata* AR4. Optimization of growth parameters for this deep-biosphere methanotroph, confirmed that it exhibited a relatively fast growth cycle and reached an optical density value of 1.6 after 72 h cultivation.

3.2. Characterization of waste streams

The characterization of solid secondary waste from CRUDE process (CSRM) showed COD, NH₄ $^+$, and VS concentration of $19.6\,\mathrm{g\,L}^{-1}$, $644\pm56\,\mathrm{mg\,L}^{-1}$ and 71.7 ± 4.5 (% w/w), respectively (Table 1). The concentrations of elemental C, H, and N- were 48.9, 7.44, and 5.05%, respectively. The CSRM subjected to TAD reactor contained 5.36 (% w/w) of reducing sugars compared to 3.32 (% w/w) present in residual liquid stream. Presence of sugars initially, in the residual streams, supported the microbial growth for performing the methanogenesis (Xia et al., 2013).

A high concentration (11.2 mg g $^{-1}$) of volatile fatty acids (VFA) was observed in the residual liquid stream of the CRUDE process. Presence of residual VFA in liquid stream is advantageous for MFC reactions as their oxidation governs the flow of the electron for producing the bioelectricity (Khanal et al., 2017). The comparatively low concentration of VFA (3.36 mg g $^{-1}$) in the CSRM was favourable for the TAD process, acidic conditions inhibited the growth of TMC. Efficient fermentation of the sugars to ethanol at the CRUDE stage resulted in low concentrations of the reducing sugars in both solid and liquid residual streams.

3.3. Thermophilic anaerobic digestion (TAD)

Results from empirical trials revealed that the highest methane yield

Table 1Degradation of FW sample across different stages of biological process.

Stage	C ₀ (g DW L ⁻¹)	IT (d)	T (°C)	COD (g L ⁻¹)		COD R.E. (%)	NH_4^+ $(mg L^{-1})$	VS (% w/w)	
				Initial	Final			Initial	Final
CRUDE	200	7	65	35.9 ± 4.4	28.1 ± 3.3	20.8 ± 3.2	644 ± 56	67.4 ± 3.3	73.1 ± 4.1
TAD	10	17	60	19.6 ± 3.8	13.8 ± 4.1	29.6 ± 2.9	224 ± 42	71.7 ± 4.5	79.7 ± 3.9
MFC	ND	42	35	25.3 ± 0.52	1.43 ± 0.35	94.3 ± 1.04	332 ± 61	ND	ND
BioGTL	ND	1	30	11.6 ± 2.9	10.3 ± 3.3	11.2 ± 2.6	119 ± 32	ND	ND

ND: Not determined

 C_0 : total carbon loaded initially in gram dry weight per liter; IT: incubation time in days; T: temperature in degree Celsius; COD: Chemical oxygen demand in gram per liter; COD R.E.: percentage reduction efficiency of a particular stage with respect to chemical oxygen demand; NH_4^+ : ammonium ions concentration in milligram per liter of liquid phase; VS: volatile solids in grams per gram of substrate loaded.

was obtained with 2% (w/v) substrate loading and an inoculum density of $10\,\mathrm{mg}\,\mathrm{L}^{-1}$ (dry cell weight). All the TAD studies were carried out under fed-batch mode for up to 30 days. After 17 days incubation, the peak methane yield from CRUDE solid residual material (CSRM) was measured (95 \pm 7 L kg⁻¹ VS). The yield was comparable to yield from raw FW (92 \pm 11 L kg⁻¹ VS). We attribute the better performance of the CSRM to the hydrolysis of the FW through the biological action of the Thermoanaerobacter sp., in the CRUDE reactor suggesting it's role as a pretreatment step prior to the TAD. In the mature reactor, the headspace was primarily methane (89 \pm 6%) and the remainder was mixture of CO₂ and N₂. The specific methane yield (SMY) and energy efficiency (EE_{TAD}) of the TAD process were 4.32 \pm 0.52 mL kg⁻¹ VS and 12.9 ± 1.74, respectively. Operational parameters were optimized through "one-variable-at-a-time" approach. High operational temperature (> 50 °C) is required to perform the anaerobic digestion under thermophilic conditions. High temperature and similar pH range was also reported in previous studies related to TAD (Areli et al., 2018).

The pH of the WWTP effluent was 5.8 and COD was 23.4 \pm 3.1 g L⁻¹. Volatile solids concentration was 71.7 \pm 4.5 (% w/ w). The methane yield at high temperature (47 L kg⁻¹ VS at 60 °C) was greater than the mesophilic condition (17 Lkg⁻¹ at 37 °C) tested. Similarly, pH 7.5 (58 L kg⁻¹ VS), 2% (w/v) substrate loading (67 L kg⁻¹ VS), 10% (v/v) inoculum density (84 L kg⁻¹ VS), and 100 RPM (89 L kg -1 VS) had profound effect on consortium growth and subsequent methane production. Low C/N ratio (6.19-7.09; compared to fermentation stage of CRUDE process) of CSRM fed to TAD revealed suitability of substrate. Observed rate of methane production is significantly higher than other recently published reports on methane production using municipal waste under thermophilic conditions. Kumar et al. (2016) had reported 0.62 Lg^{-1} COD methane production after 60 days, whereas Chakraborty and Venkata Mohan (2018) had reported a yield of 226.86 mL ${\rm g}^{-1}$ VS after 35 days using a combination of food waste and vegetable waste (Kumar et al., 2016; Chakraborty and Venkata Mohan, 2018).

The degradation capability of the TAD process was evaluated by the decrease in particulate COD (pCOD) concentration during process. The TAD stage consumed a modest fraction of the relatively low concentration of pCOD (Table 1). This can be correlated with the fact that separation of CRUDE residual material into two different solid and liquid phases reduces the overall COD loading and corresponding increase in removal efficiency at the TAD step.

The CSRM and UCE feedstocks have high levels of nitrogen compared to the FWs used for fermentation stage in CRUDE process. Ammonium (NH $_4$ ⁺) inhibits methanogens at concentrations above 1.7 g L $^{-1}$ (Inglesby and Fisher, 2012). To minimize NH $_4$ ⁺ levels, low substrate loading rates fed the TAD reactor. At the CRUDE stage, significant concentration of NH $_4$ ⁺ were present in the liquid phase as product from anaerobic microbial catalysis. As shown in Table 1, the CRUDE reactor removed nearly 68% of NH $_4$ ⁺ from the FW. Removal of significant concentration of NH $_4$ ⁺ ions at CRUDE stage further confirmed the pre-treatment effect on FW, prior to the TAD experiments. This also provides rationale for the higher titre of methane production with the CSRM compared to the raw FW.

3.4. Electricity production using MFC

A repeatable performance of the test MFCs during the two consecutive cycles suggest the use of UCE as the feedstock in the MFCs (Table 2). Per maximum power transfer theory which confirmed that maximum power can be availed from a fuel cell by choosing the external resistance ($R_{\rm ext}$) that matches the internal resistance, an external resistance of $1000\,\Omega$ was achieved. The EIS analysis suggests that the polarization losses in the MFCs fed with the CRUDE effluent decreased by 97% during the 50 days of the fed-batch operation (Table 2). The initial COD (sCOD_{in}) in the CRUDE effluent was primarily due to the monosaccharides (arabinose, fructose, galactose, glucose, sucrose, and

Table 2
Summary of the MFC experimental results.

	Cycle I	Cycle II	Cycle III
Days	500	11	41
Initial pH	7 ± 0.9	7.2 ± 0.11	7.17 ± 0.01
Final pH	4.35 ± 0.02	6.49 ± 0.03	6.7 ± 0.02
Peak power density (mW/m ²)	397.94 ± 94	551.7 ± 44	347.4 ± 15
Peak Current density (mA/m ²)	1017.15 ± 89	1893.6 ± 44	638.81 ± 58
COD removal %	18 ± 10	40 ± 21	95 ± 1
Coulombic Efficiency (%)	19 ± 1	11 ± 2	61 ± 2
Ohmic Losses (R_{Ω}) ($K\Omega$.cm ²)	0.19 ± 0.07	0.039 ± 0.01	0.074 ± 0.03
Polarization Losses (R_{ct}) ($K\Omega$.cm ²)	0.28 ± 0.11	0.977 ± 0.19	0.069 ± 0.03

xylose), fatty acids (lactic acid, vanillic acid, gallic acid, ferulic acid) and ethanol (Table 1). Considering that the organic strength in the CRUDE effluent (sCOD_{in} = 28 g COD L^{-1}) is 10-28 fold higher than that in the typical substrates used in the prior MFC studies (Ge et al., 2013), it is worth noting the efficiency exhibited by the MFCs. They removed 94% of the sCOD with a corresponding coulombic efficiency of 61% (Fig. 2a). The MFCs reduced the sCOD from $25.3\,\mathrm{g\,L}^{-1}$ to 1.43 g L⁻¹ (Table 2). As anticipated, the electrochemical output of the test MFCs increased on a temporal scale due to the increasing biocatalytic activity and decreasing charge transfer resistance on the anode surface. Results confirmed that the R_{CT} in Cycle II was an order of magnitude lower when compared to that in Cycle I (Table 2). The results also suggest that the performance of the test MFCs (fed with the CRUDE effluent) (0.56 W.m⁻²; 1.9 A.m⁻²) is on par with that fed with the pure substrates such as acetate (0.6 W.m⁻²; 1.75 A.m⁻²) (Shrestha et al., 2016). Increased values of standard error for Cycle III justified the correlation between sCOD values with adapted microbial population in mature MFC (Fig. 2a). This variation had a minimal influence on the electrical performance of the MFCs. As shown in Fig. 2b, the values of the standard errors for the power density are consistently on a lower side (< 1%) for the entire range of current density. This indicates the repeatable electrical performance of the MFCs. The conclusion regarding the minimal uncertainty of the MFC performance can be further corroborated by observing that the standard errors for the lactate, acetate, and butyrate concentration were within 1% (Fig. 2e). The minimal variation in the errors can be attributed to the chromatography parameters related to the factors including incomplete separation, peak overlapping because of non-optimized selectivity, and non-linear behavior of the detector.

The HPLC analysis reveals that the effluent in the test MFCs is characterized by the volatile fatty acids (VFAs) including lactate, acetate, and butyrate. The sum of the sCOD contributions from these three VFAs did not match the experimentally determined value for the total sCOD. These results indicate the presence of uncharacterized metabolites in the effluent that contribute to the sCOD. Nevertheless, the results confirm 98% decrease in lactate and the corresponding increases in acetate and butyrate by 48% and 74%, respectively (Fig. 2e). Slow reaction kinetics associated with colloidal particulates and complex organic matters, governed the treatment efficiency of MFCs (Nam et al., 2010). Very limited information is available on MFC operations, utilizing liquid organic waste of thermophilic fermentation process. However, the sCOD removal efficiency (95%) in current report is on par in comparison to previous studies, utilizing the effluents from mesophilic fermentation reactors.

Cyclic voltammetry analysis indicates the presence of a diffusible, redox-active species on electrochemical processes related to sCOD oxidation in the test MFCs (Fig. 2d). The redox peak lies in the range of -0.133 to -0.403 V (Vs Ag/AgCl). A series of electroanalytical studies (e.g., square wave voltammetry and differential pulse voltammetry) and chromatography studies (liquid chromatography–mass spectrometry, electrochemically controlled liquid chromatography) are

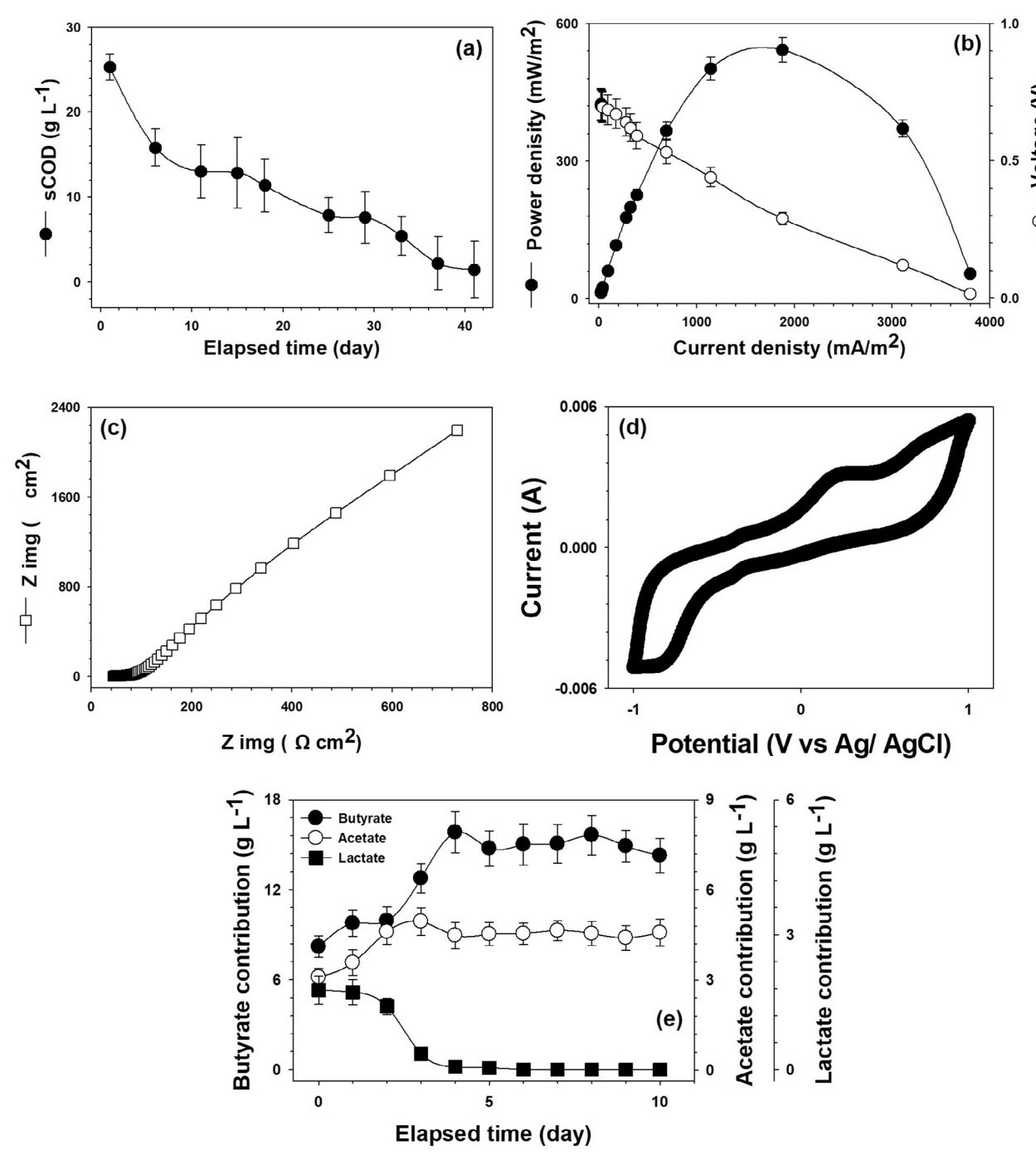


Fig. 2. Electrochemical response of a MFC for treating CRUDE effluent. (a) COD removal pattern; (b) Power density curve; (c) Nyquist plot; (d) Cyclic voltammogram; and (e) Profiles of lactate, acetate, and butyrate. Fig. 2a: sCOD vs time is based on Cycle III, biofilm age = 545 days of the microbial fuel cell (MFC). Remaining graphs are based on Cycle II, biofilm age = 531 days; Fig. 2b: Black circle represent polarization curve and white circle represent power density curve obtained by varying the external resistance from 1 to 10,000 Ω across the microbial fuel cell (MFC); Fig. 2c: Nyquist plot for MFC obtained by varying frequency range from 10,000 to 0.01 Hz using potentiostat. Fig. 2d: cyclic voltammetry curve obtained for MFC. Fig. 2e: Profiles of lactate, acetate, and butyrate.

required to characterize the intermediate redox reactions and corresponding electron transfer kinetics that affect the biological oxidation of the sCOD in the MFCs.

3.5. Methane oxidation using a deep biosphere methanotroph

Unlike chemical processes that are used to oxidize methane into methanol using the chemical catalysts (Ab Rahim et al., 2013), the present study compared methane oxidation (to methanol) for a methanotroph isolated from deep biosphere, *M. stellata*, and the archetypal methanotroph, *M. trichosporium* OB3b. Preliminary results revealed that

strain OB3b would not grow using the biogas obtained from the TAD process, presumably due to inhibitory by-products in the source (Cornish et al., 1984). Strain OB3b grew well using industrial grade methane and provided material for control experiments. All the preliminary experiments were carried out using the high inoculum concentration (1.8 g DW L $^{-1}$), 30 °C, and neutral pH conditions. After 16 h of incubation using 1.25X NMS media, the methanol concentration obtained using *M. stellata* was 0.042 mM compared to 0.127 mM obtained through *M. trichosporium* OB3b. In general, biochemical oxidation of methane was carried out under ambient conditions (Duan et al., 2011), similar to optimized parameters of current study. Selected

Table 3Variations in methanol dehydrogenase activity observed with different concentrations of inhibitors.

Concentration (mM)	MDH (U mL ⁻¹) ^a	MDH (U mL ⁻¹) ^b	MDH (U mL ⁻¹) ^c
1	0.616	0.769	0.562
2	0.447	0.483	0.456
5	0.348	0.367	0.388
10	0.114	0.152	0.207
12	0.111	0.148	-

Experiments were performed with $6\,\mathrm{mg}\,\mathrm{L}^{-1}$ cell density of *M. stellata* at 30 °C and at pH 7.0. Activity of methanol dehydrogenase in control experiment was 0.829.

- a In presence of MgCl₂.
- b In presence of NH₄Cl.
- ^c Equal concentration of each inhibitor was added to the reaction mixture.

physical parameters could be correlated with the optimal catalytic activity of methane monooxygenase enzyme of the *M. stellata*.

For increasing the methanol titer, conditions were changed to inhibit the methanol dehydrogenase (MDH) activity, as MDH quickly converts produced methanol into other cellular metabolites viz. formaldehyde. Complete inhibition of the MDH could not be targeted as such chemicals (e.g., cyclopropane etc.) would restrict the microbial uptake of substrate as well as inhibit the sMMO activity (Sheets et al., 2016). Hence precise concentration of inhibiting chemical would be maintained without disturbing the sMMO activity or limiting the methane uptake rate. Based on prior MD studies on Mg²⁺ and NH₄⁺ ions, different concentration of MgCl2 and NH4Cl were tested for inhibiting the MDH activity of M. stellata cultures (Reddy and Bruice, 2004) (Table 3). The 10 mM MgCl₂ supplement achieved highest MDH inhibition efficiency compared to the other combinations (Table 3). Though the highest inhibition of MDH activity was observed with 12 mM MgCl₂ concentration but due to cost economics and to avoid the sMMO enzyme inhibition, 10 mM concentration was selected. MDH inhibition was resulted an increase of more than 2-fold in final methanol yield and resulted in 0.089 mM of methanol under optimized conditions. Additional concentration of Mg²⁺ ion may disrupt the cofactor binding domain of the MDH enzyme thus leads to the inhibition of enzyme activity. The result is consistent with the previous reports that show Mg⁺ inhibits MDH activity (Duan et al., 2011). The NH₄Cl did not inhibit MDH significantly (Table 3). It might be due to fact that competitive inhibition caused by NH₄⁺ with substrate is not strong enough to block the substrate uptake and hence less significant inhibition was observed (Reddy and Bruice, 2004). Moreover, when MgCl₂ and NH₄Cl were combined (5mM each), no significant inhibition was observed in MDH activity. Failure of combination of MgCl2 and NH₄Cl could be attributed to not enough concentration of Mg²⁺ ions to disrupt the cofactor binding site of the MDH enzyme. Therefore, only MgCl2 was used as inhibitor.

3.6. Mass balance and energy calculations

The biochemical reactions, which include microbial growth and complex feedstock, stoichiometry information about the carbon and energy sources consumed and metabolic products formed is crucial for sustainability of the process (Gulhane et al., 2016). As per Lavoisier principle of matter, total mass of every element (C, H, N etc.) remains constant throughout different biochemical phases of reaction, therefore it was considered that available sugars (hexose and pentose) were extracted through microbial catalysis (Tambone et al., 2017). Compositional analysis confirmed the presence of insignificant amount of the insoluble solids in the reaction medium (Table 4), hence no mass loss (via evaporation) equation was applied with reaction volume corrections (Hatzis et al., 1996).

In degradation processes involving high substrate loading (like current study), failing to account for suspended insoluble solids can bias

mass balance closure and the determined concentration of main products. Therefore, C-mol values (Table 4) were used over determination of dry weight calculations (Fig. 3; Table 4). C-mol can be defined as the amount or sample of a chemical substance that contains as many elementary entities, e.g., atoms, molecules, ions, electrons, or photons, as there are atoms in one-mole of carbon-12 (¹²C). The advantage of using C-mol as the basis for calculations is that the C-mol ratio of various components within one phase of components reflects the distribution of carbon within that particular phase. Total recovery of non-reacting components was calculated as the fraction of initial carbon in separate solid and liquid phases during all the biochemical (CRUDE, TAD, MFC) processes (Hatzis et al., 1996).

Solubilization and subsequent fermentation of sugars during CRUDE process resulted in insignificant values of %C for glucose (1.66) and xylose (0.761) in CSRM. Observation of 18.9%C in CSRM compared to 39.3%C in unprocessed CRUDE effluent confirmed the solubilization of the feedstock which highlighted the efficiency of microbial hydrolysis during CRUDE process (Table 4). This further highlights the suitability of unprocessed CRUDE effluent as feedstock for MFC reaction as nearly 40% carbon is present in unprocessed CRUDE effluent as a substrate. Overall accounting of an approximately 11.6 %C as acids (acetic, lactic, gallic, ferulic, butyric acid etc.), in unprocessed CRUDE effluent was considered as stimulator for oxidation during bioelectricity production at MFC stage.

At TAD stage, ethanol is not the primary product, it constitutes only 0.185% of total carbon which corresponds to only 0.005C-mol (Table 4). Glucose is acting as the primary substrate for methane production and constitutes 1.08% of carbon at the TAD stage. High concentration of %C in the form of vanillic acid (3.05%C), gallic acid (3.58%C), and ferulic acid (2.05%C) confirmed the presence of phenolic fermentation inhibitors in solid substrate at the TAD stage (Table 4). As MFC utilized VFAs for bioelectricity generation, therefore, overall recovery of lactic acid, butyric acid, and acetic acid were 0.027, 0.029, and 0.035C-mol, respectively. Total %C recovered after MFC for all observed VFAs was only 3.63% (Table 4).

Lignin was not included in the material balance and no thermochemical pretreatment was carried out which may cause its release into the reaction mixture. Any loss of fermentable carbon, either in the form of sugar degradation products or as part of unused hydrolysate, was also accounted for, hence only 90.5% carbon in FW was accounted for in the overall process (Table 4). The approximate difference of 10% in accounting for carbon (compared to 100% carbon feed to the process) does not represent the carbon loss during the biochemical processes. This difference represents the amount of carbon that was not recovered during the stream separation, or was converted to an unidentified form (not detected through HPLC or GC analysis). Significant recovery of %C in feed after all the stages confirmed the operational efficiency and reproducibility of the developed methodology.

As per energy calculation equation (Section 2.5), heat of combustion and volatile solids in substrate were governing the overall energy withdrawal from organic waste. As energy sources are transformed to different end products (viz. ethanol, methane, methanol etc.), the concentration and specific energy values were considered for each product. After CRUDE process the values of total energy recovered was highest and followed by TAD and MFC. The overall value of energy recovered through different interrelated biochemical processes (i.e. CRUDE, TAD, and MFC) using FW as substrate was 14.8 kJ L⁻¹ per kg of VS. Oxidation of methane to methanol was not included in overall energy calculations as methanol is not directly derived from FW. This is the first report which involves the calculation of different forms of energy obtained from FW as a substrate at various stages of the biochemical processes. Further integration of CRUDE process and TAD as integrated thermophilic reactor (ITR) will provide the solution to buildup the sustainable approach of waste management. This ITR would also serve as a "one-step-one-reactor" approach for activities where space, capital investment and trained personnel is limited. Similarly, re-

Table 4
Total and overall recovery of C-mol and % Carbon in feed at different biochemical stages.

Component	Initial	Initial	Recovered				Recovered				Total recovery	
	C-mol	%C	C-mol ¹	C-mol ²	C-mol ³	C-mol ⁴	%C ¹	$%C^{2}$	%C ³	%C ⁴	C-mol	%C
Glucose	0.723	27.9	0.043	0.113	0.028	0.072	1.66	4.35	1.08	2.83	0.256	9.93
Xylose	0.596	23.1	0.020	0.069	0.011	0.036	0.761	2.65	0.425	1.41	0.135	5.25
Sucrose	0.293	11.3	0.014	0.034	0.010	0.032	0.529	1.31	0.380	1.18	0.089	3.39
Fructose	0.237	9.17	0.022	0.028	0.018	0.032	0.864	1.09	0.696	0.92	0.101	3.57
Arabinose	0.222	8.59	0.027	0.034	0.022	0.039	1.04	1.31	0.864	1.04	0.122	4.25
Galactose	0.277	10.7	0.021	0.015	0.017	0.029	0.799	0.567	0.657	0.458	0.081	2.57
Acetic acid	0.037	1.44	0.028	0.043	0.025	0.035	1.08	1.66	0.980	1.41	0.131	5.13
Lactic acid	0.005	0.206	0.018	0.078	0.016	0.027	0.709	3.02	0.606	1.06	0.139	5.39
Butyric acid	0	0	0.013	0.057	0.010	0.029	0.510	2.21	0.369	1.16	0.109	4.25
Vanillic acid	0.053	2.06	0.087	0.058	0.079	0.073	3.37	2.22	3.05	2.05	0.297	10.7
Gallic acid	0.095	3.67	0.121	0.054	0.093	0.083	4.68	2.11	3.58	1.23	0.351	11.6
Ferulic acid	0.044	1.71	0.061	0.064	0.053	0.55	2.37	2.47	2.05	2.14	0.233	9.03
Ethanol	0	0	0.014	0.371	0.005	0.009	0.555	14.3	0.185	0.388	0.399	15.4
Total	2.584	100	0.489	1.02	0.386	1.39	18.9	39.3	14.9	17.3	2.443	90.5

C-mol: amount (mass) of a substance containing 1 mol of the elemental carbon (g); number of C-mol of a component x in solid or liquid phase is calculated as $Q_x f_s / (CMW)_x$ and $[C_x] V_L / (CMW)_x$; composition of a component in the solid and liquid stream are converted to C-mol/g slurry as $Q_x f_s / CMW$ and $[C_x] (1 - f_s) / d_L (CMW)_x$; %C in feed is the ratio of total C-mol in solids or liquid stream over the total C-mol in the raw substrate; fermentation volume adjustments account for gain in mass owing to media addition during hydrolysis and are 0.9 and 0.88 g polymer/g monomer for hexose and pentose respectively.

C-mol¹, C-mol², C-mol³ and C-mol⁴ denotes value of C-mol in solid phase after CRUDE step, in liquid phase after CRUDE step, in total residual material after TAD step and in total residual material after MFC step, respectively. %C¹, %C²; %C³ and %C⁴ denoted total concentration of carbon as feed in solid phase after CRUDE step, in liquid phase after CRUDE step, in total residual material after TAD step and in total residual material after MFC step, respectively.

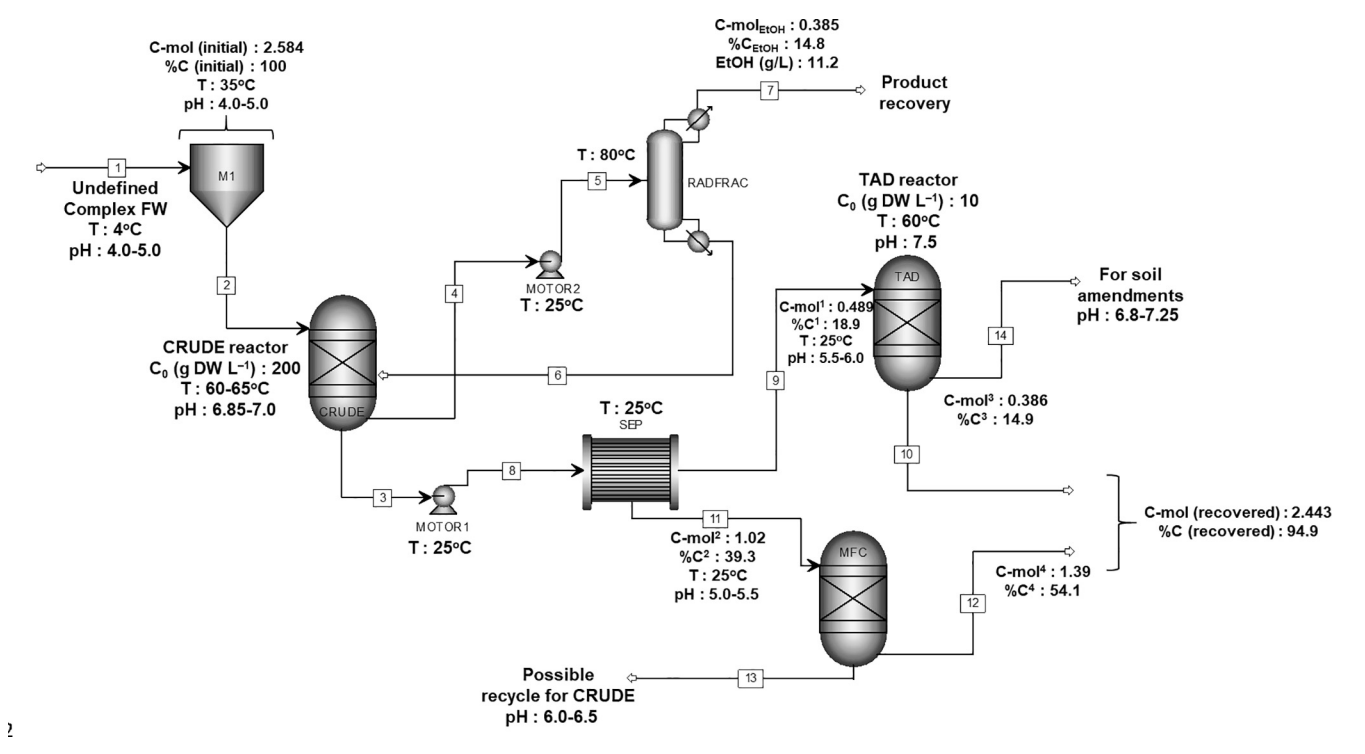


Fig. 3. An overview of the material balancing at different stages of bioprocessing in current study. C-mol¹, C-mol², C-mol³ and C-mol⁴ denotes value of C-mol in solid phase after CRUDE step, in liquid phase after CRUDE step, in total residual material after TAD step and in total residual material after MFC step, respectively. %C¹, %C², %C³ and %C⁴ denoted total concentration of carbon as feed in solid phase after CRUDE step, in liquid phase after CRUDE step, in total residual material after TAD step and in total residual material after MFC step, respectively. M1: Food waste storage, SEP: separator of solid and liquid stream after CRUDE process; RADFRAC: type of column considered for techno-economic analysis.

routing of MFC liquid residual as CRUDE nutrient supplement will also support the sustainability approach of the developed process.

4. Conclusions

This report demonstrates harvesting different forms of bioenergy from unprocessed FW by conceptualizing the fundamentals of release of minimal organic load to the environment. Utilization of CRUDE process

residual materials for biological generation of methane, electricity, and methanol broadened the product range with improved process yield. Residual MFC stream is rich in sugars which could be recycled as carbon and water supply. Channeling of FW for power generation will strengthen the green energy production efforts worldwide. All these highlights make the designed interrelated biochemical process to qualify as Green Technology.

Measurement units

Carbon loaded (C₀) – g DW L⁻¹; Incubation time – day; Temperature – °C; COD – g L⁻¹; COD reduction efficiency – %; Methane gas – mg g⁻¹ VS; Microbial inoculum – g DW L⁻¹; Peak power density – mW/m²; Peak Current density – mA/m²; COD removal – %; Coulombic Efficiency – %; Ohmic Losses (R_Q) – K Ω .cm²; Polarization Losses (R_c) – K Ω .cm²; Steady state cell voltage – V; Steady state current – A L⁻¹ d⁻¹; MDH – U mL⁻¹; Number of C-mol of a component in solid or liquid phase is calculated as Q_xf_s/(CMW)x and [C_x] V_L/(CMW)_x; composition of a component in the solid and liquid stream are converted to C-mol/g slurry as Q_xf_s/CMW and [C_x] (1 – f_s)/d_L (CMW)_x; %C in feed is the ratio of total C-mol in solids or liquid stream over the total C-mol in the raw substrate; VS – % w/w; m_s is mass of insoluble solids (g); Q_x is mass fraction of component x.

Acknowledgements

This research was supported by the US Air Force under Biological Waste to Energy Project (FA4819-14-C-0004). Financial support was also provided by the National Science Foundation in the form of *BuG ReMeDEE* initiative (Award # 1736255). Authors also acknowledge the financial support in the form of "Proof of Concept" and CNAM/Bio Centre provided by the South Dakota Governor's Office of Economic Development. Research support from the Department of Chemical and Biological Engineering at the South Dakota School of Mines and Technology is gratefully acknowledged.

Appendix A. Supplementary data

Supplementary data associated with this article can be found, in the online version, at https://doi.org/10.1016/j.biortech.2018.02.128.

References

- Ab Rahim, M.H., Forde, M.M., Jenkins, R.L., Hammond, C., He, Q., Dimitratos, N., Lopez-Sanchez, J.A., Carley, A.F., Taylor, S.H., Willock, D.J., Murphy, D.M., Kiely, C.J., Hutchings, G.J., 2013. Oxidation of methane to methanol with hydrogen peroxide using supported gold-palladium alloy nanoparticles. Angew. Chem. Int. Ed. 52, 1280–1284
- American Public Health Association, Standard methods for the examination of water and wastewater. In: Andrew D. Faton, Mary Ann H. Franson (Eds.), 1999, pp. 2–10.
- Areli, V., Begum, S., Anupoju, G.R., Kuruti, K., Shailaja, S., 2018. Dry anaerobic co-digestion of food waste and cattle manure: impact of total solids, substrate ratio and thermal pre-treatment on methane yield and quality of biomanure. Bioresour. Technol. http://dx.doi.org/10.1016/j.biortech.2018.01.050.
- Bowman, J.P., Sayler, G.S., 1994. Optimization and maintenance of soluble methane monooxygenase activity in *Methylosinus trichosporium* OB3b. Biodegradation 5, 1–11.
- Chakraborty, D., Venkata Mohan, S., 2018. Effect of food to vegetable waste ratio on acidogenesis and methanogenesis during two-stage integration. Bioresour. Technol. http://dx.doi.org/10.1016/j.biortech.2018.01.051.
- Combs, N., Hatzis, C., 1996. Development of an Epi-fluorescence assay for monitoring yeast viability and pretreatment hydrolysate toxicity in the presence of lignocellulosic solids. Humana Press Inc.
- Cornish, A., Nicholls, K.M., Scott, D., Hunter, B.K., Aston, W.J., Higgins, I.J., Sanders, J.K.M., 1984. In vivo ¹³C NMR investigations of methanol oxidation by the obligate methanotroph *Methylosinus trichosporium* OB3b. Microbiology 130, 2565–2575.
- Dhiman, S.S., David, A., Braband, V.W., Hussein, A., Salem, D.R., Sani, R.K., 2017a. Improved bioethanol production from corn stover: role of enzymes, inducers and simultaneous product recovery. Appl. Energy 208, 1420–1429.
- Dhiman, S.S., David, A., Shrestha, N., Johnson, G.R., Benjamin, K.M., Gadhamshetty, V., Sani, R.K., 2017b. Simultaneous hydrolysis and fermentation of unprocessed food waste into ethanol using thermophilic anaerobic bacteria. Bioresour. Technol. 244, 733–740
- Dhiman, S.S., Haw, J.-R., Kalyani, D., Kalia, V.C., Kang, Y.C., Lee, J.-K., 2015.
 Simultaneous pretreatment and saccharification: green technology for enhanced sugar yields from biomass using a fungal consortium. Bioresour. Technol. 179, 50–57.
- Dhiman, S.S., Jagtap, S.S., Jeya, M., Haw, J.-R., Kang, Y.C., Lee, J.-K., 2012. Immobilization of *Pholiota adiposa* xylanase onto SiO₂ nanoparticles and its application for production of xylooligosaccharides. Biotechnol. Lett. 34, 1307–1313.
- Dhiman, S.S., Kalyani, D., Jagtap, S.S., Haw, J.-R., Kang, Y.C., Lee, J.-K., 2013. Characterization of a novel xylanase from *Armillaria gemina* and its immobilization onto SiO₂ nanoparticles. Appl. Microbiol. Biotechnol. 97, 1081–1091.
- Dhiman, S.S., Selvaraj, C., Li, J., Singh, R., Zhao, X., Kim, D., Kim, J.Y., Kang, Y.C., Lee, J.-

- K., 2016. Phytoremediation of metal-contaminated soils by the hyperaccumulator canola (*Brassica napus* L.) and the use of its biomass for ethanol production. Fuel 183, 107–114.
- Duan, C., Luo, M., Xing, X., 2011. High-rate conversion of methane to methanol by Methylosinus trichosporium OB3b. Bioresour. Technol. 102, 7349–7353.
- Food Waste: The Facts. Regional Office of North America: United Nations Environment Programme, 2015.
- Gancedo, C., Serrano, R., 1989. Energy-yielding metabolism. In: Rose, A.H., Harrison, J.S. (Eds.), The Yeasts, 2nd ed. Academic Press London, England, pp. 205–259.
- Ge, Z., Zhang, F., Grimaud, J., Hurst, J., He, Z., 2013. Long-term investigation of microbial fuel cells treating primary sludge or digested sludge. Bioresour. Technol. 136, 509–514
- Gulhane, M., Khardenavis, A.A., Karia, S., Pandit, P., Kanade, G.S., Lokhande, S., Vaidya, A.N., Purohit, H.J., 2016. Biomethanation of vegetable market waste in an anaerobic baffled reactor: effect of effluent recirculation and carbon mass balance analysis. Bioresour. Technol. 21, 100–109.
- Gustavsson, J., Sonesson, U., van Otterdijk, R., Meyback, A., 2011. Global Food Losses and Food Waste: Extend, Causes and Prevention at Interpack, Düsseldorf, Germany.
- Hatzis, C., Riley, C., Philippidis, G., 1996. Detailed material balance and ethanol yield calculations for the biomass-to-ethanol conversion process. In: Wyman, Charles E., Davison, B.H. (Eds.), Seventeenth Symposium on Biotechnology for Fuels and Chemicals. Humana Press, New York, USA, pp. 443–459.
- Inglesby, A.E., Fisher, A.C., 2012. Enhanced methane yields from anaerobic digestion of Arthrospira maxima biomass in an advanced flow-through reactor with an integrated recirculation loop microbial fuel cell. Energy Environ. Sci. 5, 7996–8006.
- Khanal, S.K., Giri, B., Nitayavardhana, S., Gadhamshetty, V., 2017. Anaerobic bioreactors/digesters: design and development. In: Jegatheesan, V., Ngo, H.H., Hallenbeck, P.C., Pandey, A. (Eds.), Current Developments in Biotechnology and Bioengineering. Elsevier, pp. 261–279.
- Koutinas, A.A., Vlysidis, A., Pleissner, D., Kopsahelis, N., Lopez Garcia, I., Kookos, I.K., Papanikolaou, S., Kwan, T.H., Lin, C.S.K., 2014. Valorization of industrial waste and by-product streams via fermentation for the production of chemicals and biopolymers. Chem. Soc. Rev. 43, 2587–2627.
- Lin, C.S.K., Pfaltzgraff, L.A., Herrero-Davila, L., Mubofu, E.B., Abderrahim, S., Clark, J.H., Koutinas, A.A., Kopsahelis, N., Stamatelatou, K., Dickson, F., Thankappan, S., Mohamed, Z., Brocklesby, R., Luque, R., 2013. Food waste as a valuable resource for the production of chemicals, materials and fuels. Current situation and global perspective. Energy Environ. Sci. 6, 426–464.
- Logan, B.E., Hamelers, B., Rozendal, R., Schröder, U., Keller, J., Freguia, S., Aelterman, P., Verstraete, W., Rabaey, K., 2006. Microbial fuel cells: methodology and technology. Environ. Sci. Technol. 40, 5181–5192.
- Michel, H., 2012. Editorial: the nonsense of biofuels. Angew. Chem. Int. Ed. 51, 2516-2518
- Nam, J.-Y., Kim, H.-W., Lim, K.-H., Shin, H.-S., 2010. Effects of organic loading rates on the continuous electricity generation from fermented wastewater using a singlechamber microbial fuel cell. Bioresour. Technol. 101, S33–S37.
- Perlack, R.D., Turhollow, A.F.., Graham, R.L., Stokes, B.J., Erbach, D.C., 2015. Biomass as Feedstock for a Bioenergy and Bioproducts Industry: The Technical Feasibility of a Billion-ton Annual Supply. U.S. Department of Energy & U.S., Department of Commerce.
- Rahayu, F., Kawai, Y., Iwasaki, Y., Yoshida, K., Kita, A., Tajima, T., Kato, J., Murakami, K., Hoshino, T., Nakashimada, Y., 2017. Thermophilic ethanol fermentation from lignocellulose hydrolysate by genetically engineered *Moorella thermoacetica*. Bioresour. Technol. 245, 1393–1399.
- Reddy, S.Y., Bruice, T.C., 2004. Mechanisms of ammonia activation and ammonium ion inhibition of quinoprotein methanol dehydrogenase: a computational approach. Proc Natl. Acad. Sci. 101, 15887–15892.
- Roels, J.A., 1983. Energetics and Kinetics in Biotechnology. Elsevier Biomedical, Amsterdam, The Netherlands.
- Rosentrater, K.A., 2006. A review of corn masa processing residues: Generation, properties, and potential utilization. Waste Manage. 26, 284–292.
- Sheets, J.P., Ge, X., Li, Y.-F., Yu, Z., Li, Y., 2016. Biological conversion of biogas to methanol using methanotrophs isolated from solid-state anaerobic digestate. Bioresour. Technol. 201, 50–57.
- Shrestha, N., Chilkoor, G., Xia, L., Alvarado, C., Kilduff, J.E., Keating, J.J., Belfort, G., Gadhamshetty, V., 2017. Integrated membrane and microbial fuel cell technologies for enabling energy-efficient effluent Re-use in power plants. Water Res. 117, 37–48.
- Shrestha, N., Fogg, A., Wilder, J., Franco, D., Komisar, S., Gadhamshetty, V., 2016. Electricity generation from defective tomatoes. Bioelectrochemistry 112, 67–76.
- Tambone, F., Orzi, V., D'Imporzano, G., Adani, F., 2017. Solid and liquid fractionation of digestate: Mass balance, chemical characterization, and agronomic and environmental value. Bioresour. Technol. 243, 1251–1256.
- Vohra, M.H., Jain, P., Jha, T., Sharma, M., Dureja, P., Sarma, P.M., Lal, B., 2015. Separation of acetone and butyric acid for simultaneous analysis of sugars, volatile fatty acids, acetone and alcohols by HPLC using flow programming. Anal. Methods 7, 7618–7624.
- Wu, Y., Zhao, X., Jin, M., Li, Y., Li, S., Kong, F., Nan, J., Wang, A., 2018. Copper removal and microbial community analysis in single-chamber microbial fuel cell. Bioresour. Technol. http://dx.doi.org/10.1016/ji.biortech.2018.01.046.
- Xia, A., Cheng, J., Lin, R., Lu, H., Zhou, J., Cen, K., 2013. Comparison in dark hydrogen fermentation followed by photo hydrogen fermentation and methanogenesis between protein and carbohydrate compositions in *Nannochloropsis oceanica* biomass. Bioresour. Technol. 138, 204–213.